

# Maximizing and evaluating the impact of test-trace-isolate programs

Kyra H. Grantz<sup>1\*</sup>, Elizabeth C. Lee<sup>1\*</sup>, Lucy D'Agostino McGowan<sup>2</sup>, Kyu Han Lee<sup>1</sup>, C. Jessica E. Metcalf<sup>3,4</sup>, Emily S. Gurley<sup>1</sup>, and Justin Lessler<sup>1</sup>

<sup>1</sup>Department of Epidemiology, Johns Hopkins Bloomberg School of Public Health, Baltimore, MD, USA

<sup>2</sup>Department of Mathematics and Statistics, Wake Forest University, Winston-Salem, NC, USA

<sup>3</sup>Department of Ecology and Evolutionary Biology, Princeton University, Princeton, NJ, USA

<sup>4</sup>Princeton School of Public and International Affairs, Princeton University, Princeton, NJ, USA

\*denotes equal contribution

September 2, 2020

## Abstract

**Background:** Test-trace-isolate programs are an essential part of COVID-19 control that offer a more targeted approach than many other non-pharmaceutical interventions. Effective use of such programs requires methods to estimate their current and anticipated impact.

**Methods and Findings:** We present a mathematical modeling framework to evaluate the expected reductions in the reproductive number,  $R$ , from test-trace-isolate programs. This framework is implemented in a publicly available R package and an online application. We evaluated the effects of case detection, speed of isolation, contact tracing completeness and speed of quarantine using parameters consistent with COVID-19 transmission ( $R_0 = 2.5$ , generation time 6.5 days). We show that  $R$  is most sensitive to changes to the proportion of infections detected in almost all scenarios, and other metrics have a reduced impact when case detection levels are low ( $< 30\%$ ). Although test-trace-isolate programs can contribute substantially to reducing  $R$ , exceptional performance across all metrics is needed to bring  $R$  below one through test-trace-isolate alone, highlighting the need for comprehensive control strategies. Formally framing the dynamical process also indicates that metrics used to evaluate performance of test-trace-isolate, such as the proportion of identified infections among traced contacts, may be misleading. While estimates of program performance are sensitive to assumptions about COVID-19 natural history, our qualitative findings are robust across numerous sensitivity analyses.

**Conclusions:** Effective test-trace-isolate programs first need to be strong in the "test" component, as case detection underlies all other program activities. Even moderately effective

36 test-trace-isolate programs are an important tool for controlling the COVID-19 pandemic,  
37 and can alleviate the need for more restrictive social distancing measures.

## 38 Introduction

39 In the absence of a vaccine or a widely-available prophylactic drug, non-pharmaceutical inter-  
40 ventions are the only tools available to curb the spread of the ongoing COVID-19 pandemic.  
41 During the initial phases of the pandemic, broad-reaching interventions like stay-at-home orders  
42 and non-essential business closures were applied throughout the world, affecting large swathes  
43 of the population and causing severe social and economic disruption [1–6].

44 Because of the high costs of broad scale social distancing measures, there has been an  
45 increasing focus on alternative approaches with fewer ancillary costs. One such approach is a  
46 test-trace-isolate program, in which extensive *testing* is used to identify cases in the community;  
47 public health agencies then *trace* the contacts of these cases in order to identify people who may  
48 have been infected; and the initial cases are asked to *isolate* and their contacts are asked to  
49 quarantine for the period of time that they could be, or become, infectious [7]. If effective, test-  
50 trace-isolate programs can reduce the need for more restrictive, widespread control measures.  
51 Already they have played a critical role in controlling SARS-CoV-2 transmission in places  
52 ranging from Utah to South Korea, where these programs have been credited with enabling  
53 successful control while avoiding the most restrictive social distancing measures (e.g., stay-at-  
54 home orders) [8–11].

55 Not all test-trace-isolate programs are created equal, and the success of test-trace-isolate  
56 programs is ultimately measured in their ability to reduce transmission. The proportion of  
57 infections identified through testing and contact tracing dictate the proportion of transmission  
58 chains we can potentially disrupt, while the speed of isolation and quarantine dictates how  
59 many potentially infectious contacts are prevented [12]. The resulting reductions in disease  
60 transmission can be quantified and compared by estimating the reproductive number,  $R$ , the  
61 average number of new infections caused by a single infected individual.

62 Translating test-trace-isolate program metrics into reductions in the reproductive number is  
63 not a direct calculation due to feedback loops between control measures and disease transmission  
64 dynamics. As a test-trace-isolate program interrupts chains of transmission, it changes the  
65 propagation of disease in future generations. Any approach aiming to translate quantitative  
66 program metrics into meaningful measures of the effectiveness of disease control must account  
67 for these dynamic processes.

68 Here, we propose a mathematical framework for modeling the impact of test-trace-isolate  
69 strategies on onward transmission, as measured by expected reductions in the reproductive  
70 number. Using this approach, we explore the factors which most influence the success of a  
71 test-trace-isolate program, their interactions, and how these results may be used in developing  
72 strategies for improvement. To enable broad adoption of our approach, the methods presented  
73 here are implemented in an R package, **t*t*i** [13], and the web-based Contact Tracing Evaluation  
74 and Strategic Support Application (ConTESSA) [14], both of which are freely available online.

## 75 Methods

### 76 Mathematical Framework

77 To estimate the effectiveness of a test-trace-isolate program, we frame our analysis in terms  
78 of the effective reproductive number,  $R$ , defined as the number of onward transmissions an  
79 infected individual is expected to make given the current immune status of the population  
80 and implemented control measures. We first define the population of infected individuals to  
81 be spread across three compartments; infections **D**etected through testing and subsequently  
82 isolated ( $D$ ), infections among **Q**uarantined contacts of identified cases ( $Q$ ) and undetected  
83 infections in the **C**ommunity ( $C$ ) (Figure 1). Though there will be uninfected individuals both  
84 in quarantine and in the community, these do not play a role in our calculations and are ignored.

85 We consider the proportion of the population in each compartment at any given time  $t$  to be  
86 defined by a  $1 \times 3$  matrix, denoted  $DQC_t$ . To calculate the proportion of infected individuals in  
87 each compartment at time  $t + 1$ , we apply the rates at which individuals in each compartment  
88 cause new infections, and then the rates at which these secondary infections are detected and  
89 isolated through the following equation:

$$DQC_{t+1} = \frac{(DQC_t)(INFECT)(DETECT)}{\sum[(DQC_t)(INFECT)]}, \quad (1)$$

90 where  $INFECT$  is a  $3 \times 3$  diagonal matrix describing the number of infections caused in the  
91 next generation by members of each detection compartment, and  $DETECT$  is a  $3 \times 3$  matrix  
92 describing the probability that infections in the next generation are detected and isolated,  
93 quarantined, or undetected in the community.

The diagonal elements of the  $INFECT$  matrix,  $[R_D, R_Q, R_C]$ , represent the reproductive number for members of each compartment. Hence, given the normalized version of the  $DQC$  matrix specified above, we can calculate the overall reproductive number at time  $t$  as:

$$R_t = (DQC_t)(INFECT)$$

94 The  $DETECT$  matrix then assigns these new infections to the appropriate detection classes  
95 of the  $DQC$  matrix in the next generation. Specifically:

$$DETECT = \begin{bmatrix} I(D) \rightarrow D & I(D) \rightarrow Q & I(D) \rightarrow C \\ I(Q) \rightarrow D & I(Q) \rightarrow Q & I(Q) \rightarrow C \\ I(C) \rightarrow D & 0 & I(C) \rightarrow C \end{bmatrix} = \begin{bmatrix} (1 - \omega_D)\rho & \omega_D & (1 - \omega_D)(1 - \rho) \\ (1 - \omega_Q)\rho & \omega_Q & (1 - \omega_Q)(1 - \rho) \\ \rho & 0 & (1 - \rho) \end{bmatrix} \quad (2)$$

96 where  $I(X)$  represents those infected by people in compartment  $X$  in the the previous gen-  
97 eration,  $\omega_X$  is the probability that a contact of a detected individual in compartment  $X$  is  
98 traced and quarantined (quarantine completeness), and  $\rho$  is the probability that a community  
99 infection is detected and isolated by a test-trace-isolate program (isolation completeness). The  
100 transitions in each row of the  $DETECT$  matrix represent the probability that people in the  
101 corresponding notional infection compartment will be detected by a particular means (hence

102 rows sum to one).

103 The other aspect that determines the effectiveness of a test-trace-isolate program is the  
104 reduction in  $R$  that we see among those who are isolated or quarantined (Figure 2). We define  
105 the relative transmissibility of individuals in these compartments by  $\gamma_D$  and  $\gamma_Q$  such that:

$$R_D = \gamma_D R_C \quad (3)$$

$$R_Q = \gamma_Q R_C \quad (4)$$

106 The main mechanism by which isolation and quarantine reduce transmission is the (at least  
107 partial) truncation of the infectious period. Hence, these values are defined by the equations:

$$\gamma_D = \int_{-\infty}^{\tau_D} f(x) dx \quad (5)$$

$$\gamma_Q = \int_{-\infty}^{\tau_Q} g(x) dx \quad (6)$$

108 where  $f(x)$  is the distribution of relative infectiousness indexed from day of symptom onset;  
109  $g(x)$  is the expected distribution of relative infectiousness of secondary cases indexed from their  
110 infector's time of symptom onset; and  $\tau_D$  and  $\tau_Q$  represent the average time to isolation and  
111 quarantine, respectively, from time of case symptom onset.

## 112 **Translating Observed Metrics to Model Inputs**

113 Health departments collect data on their test-trace-isolate programs, but these observed metrics  
114 need to be translated into model inputs. To estimate *isolation completeness* ( $\rho$ ), we can divide  
115 the average number of infections that were isolated by the estimated number of total infections  
116 in the community. The latter value may be difficult to obtain, but can be approximated in  
117 a number of ways, including serosurveys and extrapolation from the number of deaths and  
118 approximate infection fatality ratio. *Quarantine completeness* ( $\omega$ ) can be estimated by dividing  
119 the number of quarantined individuals by the total number of contacts.

120 For the purposes of our model, *time to isolation* ( $\tau_D$ ) is the average number of days from  
121 case symptom onset to case isolation, while *time to quarantine* ( $\tau_Q$ ) is the average number of  
122 days from case symptom onset to contact quarantine. Often these timings are the composite of  
123 several constituent processes, including time from symptom onset to testing, time from testing to  
124 notification and isolation, and the time from obtaining a test result to tracing and quarantining  
125 contacts.

## 126 **Adding real-world complexity to the model**

127 Above we describe the basic model framework, but to take into account the complexities of the  
128 real world, we can expand the number of compartments in the  $DQC$  matrix and the correspond-  
129 ing *INFECT* and *DETECT* transitions. In the implementation used to generate the results  
130 described below, we create compartments to differentiate symptomatic and asymptomatic in-  
131 fections as well as household and community contacts to address the fact that these groups  
132 may differ in their probability and speed of detection, ability to be traced and quarantined,

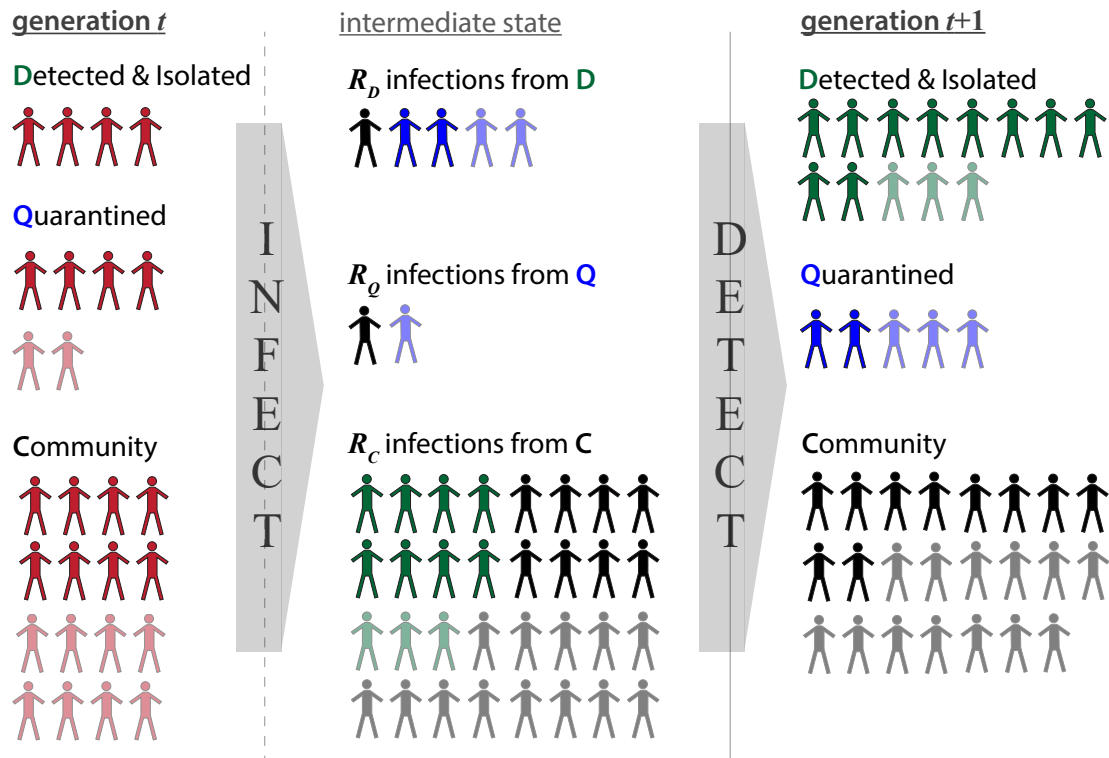


Figure 1: Conceptual representation of the model algorithm, where infections in generation  $t$  (left column) infect new individuals according to  $R_D$ ,  $R_Q$ , and  $R_C$  reproductive numbers that populate the *INFECT* matrix (center column). These newly propagated infections are then distributed into  $D$ ,  $Q$ , and  $C$  compartments in generation  $t + 1$  (right column) according to the various detection transition probabilities specified in the *DETECT* matrix (colors of center column). Symptomatic individuals (darker shading) may be more likely to be detected than asymptomatic individuals (lighter shading)

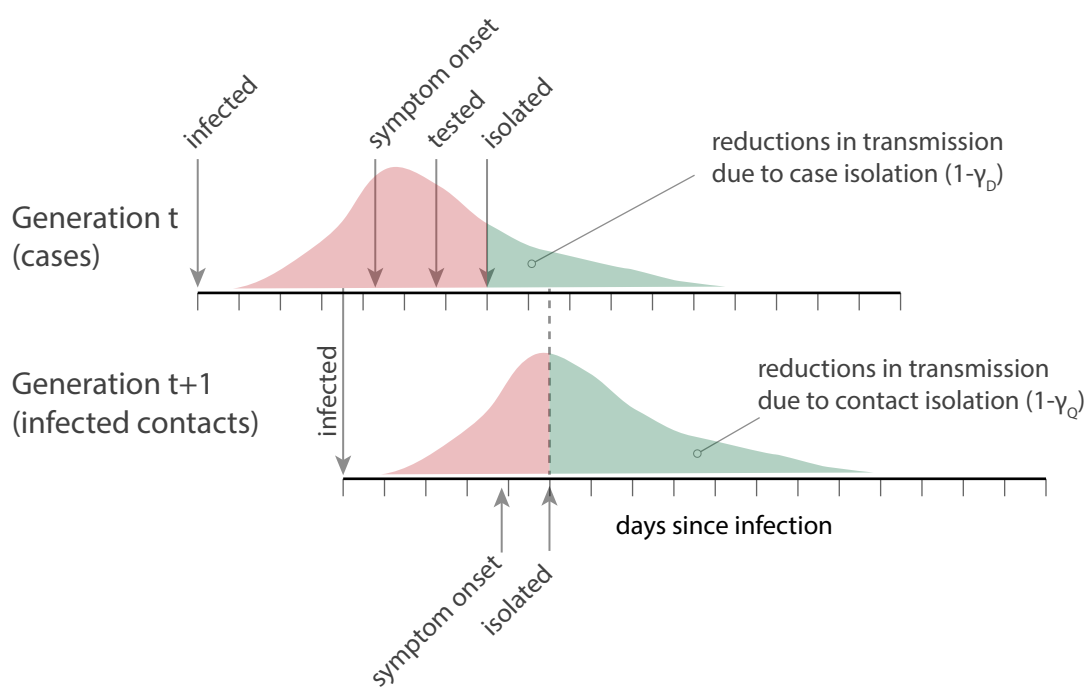


Figure 2: Conceptual representation of test-trace-isolate programs, where detection of a case in generation  $t$  through widespread *testing* and subsequent *isolation* reduces onward transmission to generation  $t+1$ . Individuals in generation  $t+1$  are then *traced* and quarantined to reduce onward transmission from those who may be infected.

133 infectiousness, and risk of being infected.

134 This expanded model has nine *DQC* compartments and is described in full in the Supple-  
135 mentary Methods.

## 136 Disease simulation

137 To obtain expected reductions in  $R$ , we first initiate the model with a *DQC* matrix that has  
138 only undetected community infections ( $C = 1$ ). Then we simulate the infection and detection  
139 processes across multiple disease generations until equilibrium is achieved in the *DQC* matrix  
140 (this usually occurs in less than ten generations). This equilibrium provides an estimate of  
141 what would be achieved by a specified test-trace-isolate strategy if it maintained its current  
142 characteristics for the foreseeable future.

143 The model may also be run as a stochastic simulation, to explore the impact of overdispersion  
144 and stochasticity in the epidemic process in general. In stochastic simulations we normalize  
145 the *DQC* matrix to a standard population size, then simulate the number of infections each  
146 individual causes for each notional *INFECT* compartment as a random draw from a negative  
147 binomial distribution based on the values in the *INFECT* matrix. These infections are then  
148 assigned to the compartments *DQC* matrix based on draws from a multinomial distribution pa-  
149 rameterized by the rows of the *DETECT* matrix. Since there is no equilibrium state, stochastic  
150 simulations are run for a fixed number of generations.

151 The simulations presented in this paper assume that  $R_0 = 2.5$  without interventions, a  
152 generation time of 6.5 days (unless otherwise stated, Table S3), and initially, that whether  
153 individuals develop symptoms or not has no meaningful impact on transmission or detection  
154 probability in surveillance, and that household and community contacts are equally likely to  
155 be infected and quarantined. In later analyses, we relax these latter assumptions and add  
156 stochasticity to illustrate how our results are influenced by overdispersion in transmission, the  
157 presence of asymptomatic transmission, and differential risk of infection and tracing speed in  
158 household contacts.

## 159 Data and model availability

160 The expanded model is implemented in the **tti** R package [13]. We also developed the Contact  
161 Tracing Evaluation and Strategic Support Application (ConTESSA), an R Shiny web applica-  
162 tion, around a simplified version of our modeling framework. The purpose of this application is  
163 to provide a user-friendly interface where managers of test-trace-isolate activities, equipped with  
164 their observed metrics, can examine how well their program reduces onward transmission and  
165 explore how their results might change with improvements to completeness and timing metrics  
166 as well as different underlying assumptions. The ConTESSA application is complemented by  
167 a free Coursera course that describes key contact tracing program metrics and provides more  
168 detailed instruction on how to use the application [15].

## 169 Results

### 170 Case isolation and contact quarantine completeness and timing

171 Application of our framework shows that the reproductive number can be reduced by improving  
172 performance across all dimensions of a test-trace-isolate program: detection and isolation com-  
173 pleteness, the speed of case isolation, the proportion of contacts followed up and quarantined,  
174 and the speed at which quarantine occurs (Figure 3). However, the effect of improvements in  
175 one dimension are not independent of performance in the other dimensions, and as such, the  
176 aspect where improvements will yield the greatest dividends, the "next best move", depends on  
177 the current status of the program.

178 Consider a situation where you only detect and isolate 10% of cases through your community  
179 testing program, and it takes an average of seven days from symptom onset to do so (squares  
180 in Figure 3). Whether you have highly effective contact tracing (70% of contacts quarantined  
181 on average 4 days after case symptom onset, hollow shapes in Figure 3) or less effective contact  
182 tracing (30% quarantined on average 8 days after case symptom onset, solid shapes in Figure  
183 3), little will be gained by improving the speed of case isolation, and the greatest reductions in  
184 transmission will be achieved by improving the proportion of infections detected and isolated  
185 (direction 1 in 3A). Increasing the proportion of infections detected and isolated, regardless of  
186 other metrics, is critical because it is these detected cases that "seed" all other test-trace-isolate  
187 activities. If an infection is not detected, it cannot be isolated, and their contacts cannot be  
188 traced and quarantined.

189 Reducing the time to case isolation (direction 2 in Figure 3A) may be nearly as effective as  
190 improving case isolation completeness in certain contexts, in particular, if contact tracing is less  
191 effective and isolation completeness is reasonably high (over 30%). Because the vast majority of  
192 transmission occurs in the days immediately before and after symptom onset, improvements in  
193 the speed of case isolation that bring it to four days or fewer will yield the greatest reductions  
194 in transmission. Beyond this, there is limited opportunity to reduce onward transmission of  
195 the isolated case and thus little difference between delays of 6, 8, or 10 days. Increasing the  
196 speed of case isolation is particularly important when contact tracing is ineffective (Figure 3B),  
197 hence the program must rely predominantly on reductions in transmission from isolated cases  
198 themselves.

199 The benefits of increasing the speed and completeness of contact tracing and quarantine are  
200 greatest in the context of already highly effective testing and isolation (e.g., 50% of infections  
201 isolated on average 4 days after symptom onset, circles in Figure 3D). In such situations,  
202 increasing quarantine completeness yields the largest reductions in transmission (direction 3 in  
203 Figure 3D), particularly when the speed of contact quarantine is less than 8 days from case  
204 symptom onset.

205 Improvements in the speed of contact quarantine (direction 4 in Figure 3D) are most effective  
206 during the 4-8 day window after case symptom onset for similar reasons; this period corresponds  
207 to the greatest expected infectiousness of infected contacts. The impact of improvements in the  
208 speed or completeness of contact tracing is less if testing and isolation fail to reach a high  
209 percentage of infections (Figure 3E). As noted above, this is because without adequate detected



210 cases to seed contact tracing activities, the ability of tracing and quarantine to have an impact  
211 is substantially reduced.

212 The completeness and timing of test-trace-isolate activities determine whether we can achieve  
213 goals in disease control using these approaches. A common goal is to bring  $R$  below one so that  
214 the epidemic will start to recede in the population. We explored the range of program charac-  
215 teristics that could achieve this goal, under the assumption that contacts were quarantined on  
216 the same day as case isolation, and quarantine completeness ranged from 50-100% (Figure 4).

217 At  $R = 2.5$  (our baseline when no other interventions are in place) with perfect contact  
218 quarantine, at least 60% of cases must be isolated to achieve  $R < 1$ ; this minimum percentage  
219 decreases to 50% when starting at  $R = 2$ , 34% at  $R = 1.5$ , and 20% at  $R = 1.25$  (corresponding  
220 to 20%, 40%, and 50% reductions in baseline  $R$  due to other interventions) (Figure 4). It is not  
221 possible to achieve  $R < 1$  if case isolation occurs more than 8.0 days after symptom onset, on  
222 average, and this threshold increases to 9, 11, and 13 days for  $R$  starting at 2, 1.5, and 1.25.

223 Quarantine need not be perfect to achieve  $R < 1$  (colors in Figure 4), but the tolerance for  
224 imperfect quarantine changes with isolation speed. For example, case isolation completeness  
225 needs to only increase from 60% to 63% to offset a decrease in contact quarantine completeness  
226 from 100% to 50% when cases are isolated on the same day as symptom onset. However, this  
227 tolerance for incomplete quarantine rapidly degrades as the time to isolation increases, and, in  
228 the absence of other interventions (i.e.,  $R = 2.5$ ), no isolation program will achieve  $R < 1$  with  
229 50% quarantine completeness if the average time to case isolation exceeds 2.6 days.

## 230 **Infections arising in traced contacts**

231 A metric often recommended for evaluating test-trace-isolate programs is the proportion of iden-  
232 tified infections that were already under quarantine [7]. Programs are thought to be successful  
233 if this metric is high because it may indicate that a substantial fraction of transmission chains  
234 were interrupted through isolation of case contacts early in (or prior to) their infectious period.  
235 In practice, a program might approximate this by calculating the proportion of all newly de-  
236 tected infections among traced contacts, who may or may not be in quarantine when they are  
237 confirmed to be infected. This proportion is equivalent to  $\frac{Q}{Q+D}$  in our model.

238 An increasing proportion of new infections detected among traced contacts only represents  
239 an improvement in the program effectiveness if the timing of case isolation remains constant or  
240 becomes quicker. As delays in isolation increase, a greater number of secondary infections will  
241 occur among traced contacts. Hence, we can see both an increase in the proportion of newly  
242 detected infections among traced contacts and an increase in the effective reproductive number  
243 (direction ‘2’ in Figure 5).

## 244 **Adding real-world complexity to transmissibility and risk**

245 In the sections above, we assume that all infected individuals are equally likely to transmit and  
246 be detected. Yet, there is evidence that asymptomatic individuals (those who never develop  
247 symptoms) are less infectious than those who do develop symptoms [16, 17]. If the relative  
248 contribution of asymptomatic individuals to onward transmission is low, limited detection of  
249 asymptomatic cases will have little effect on the reproductive number (Figure S1).

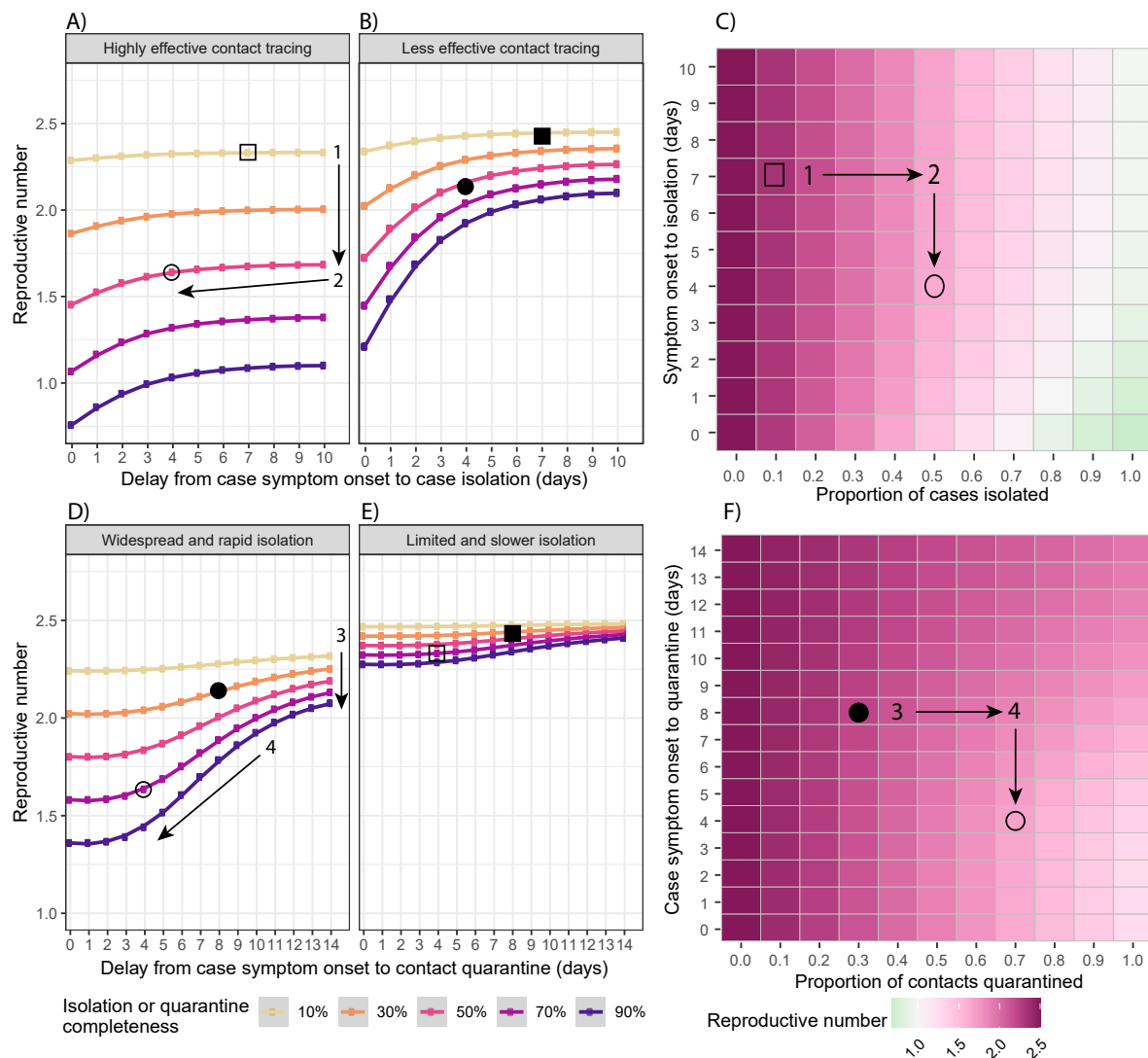


Figure 3: Improvements to case isolation and contact quarantine: Impact of case isolation timing (x-axis) and completeness (line colors) on the effective reproductive number (y-axis) for A) a highly effective contact tracing program and B) a less effective contact tracing program. C) Heat map of the effective reproductive number across a range of case isolation timing (y-axis) and completeness (x-axis) scenarios, assuming that contact tracing is highly effective. Impact of contact tracing timing (x-axis) and completeness (line colors) on the effective reproductive number (y-axis) for D) a widespread and rapid case isolation scenario and E) a less effective and slower case isolation scenario. F) Heat map of the effective reproductive number across a range of contact tracing timing (y-axis) and completeness (x-axis) scenarios, assuming that detection and isolation of index cases is widespread and rapid. For all panels, the open shapes mark example scenarios with highly effective contact tracing (70% quarantined on average 4 days after case symptom onset) in contrast to the filled shapes of a less effective contact tracing scenario (30% quarantined after 8 days). Circles mark example scenarios with widespread and rapid case isolation (50% isolated on average 4 days after case symptom onset) in contrast to squares, which have limited and slower case isolation (10% isolated after 7 days). Shapes display consistent scenarios across all panels in the figure.

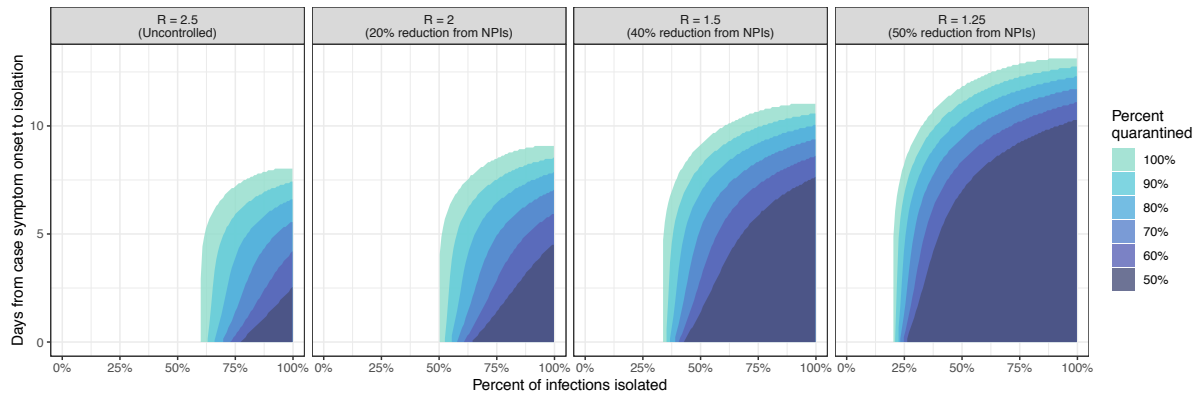


Figure 4: Isolation strategies (timing and completeness) capable of achieving  $R < 1$  when a given proportion of contacts (50 - 100%) are quarantined on the same day as case isolation. These strategies are shown for four possible baseline values of  $R$ , assuming other non-pharmaceutical interventions (NPIs) are in effect to reduce transmission from the uncontrolled scenario,  $R = 2.5$ .

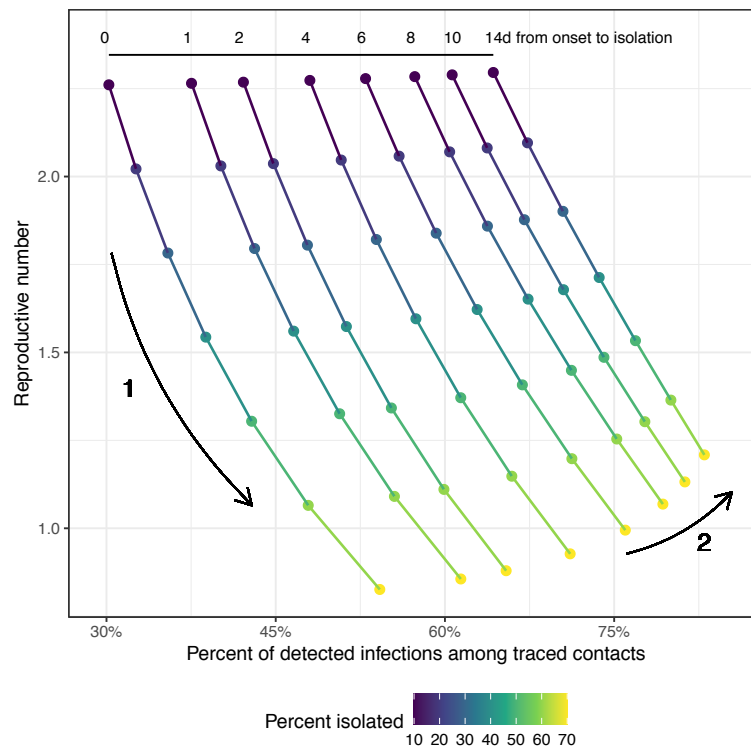


Figure 5: Relationship between  $R$  and the proportion of detected infections among traced contacts. Each position along a line shows a single test-trace-isolate strategy, with a fixed delay from case symptom onset to isolation (shown in the numbers at the top) and 90% of contacts quarantined on the same day as case isolation. Points are colored by the proportion of infections detected and isolated through testing. When isolation timing remains constant, higher case isolation completeness corresponds with increases in the proportion of detected infections among traced contacts and reductions in  $R$  (Arrow 1). However, increases in the proportion of detected infections among traced contacts could indicate an increase in  $R$ , if the delay to case isolation is also increasing, thus leading to more secondary cases among traced contacts (Arrow 2).

250 Similarly, previous scenarios assume that all contacts are equally at risk of being infected,  
251 but contact tracing studies suggest that the risk of SARS-CoV-2 infection for household contacts  
252 could be six (or more) times higher compared to other close contacts [11, 16]. Quarantining  
253 household contacts therefore is expected to have a larger impact in reducing the reproductive  
254 number than quarantining non-household contacts (Figure S2).

255 There is growing evidence that the distribution of onward transmission for SARS-CoV-2 is  
256 overdispersed, meaning that most individuals contribute little to onward transmission, while  
257 super-spreading events result in the bulk of secondary infections [18, 19]. Overdispersion has  
258 little effect on the mean estimates of the reproductive number (Figure S3). However, when there  
259 are few total infections in a community, the random occurrence or detection of any one super-  
260 spreading event can drastically alter program impact, including ending an outbreak altogether,  
261 thereby increasing uncertainty in  $R$ .

## 262 Sensitivity Analyses

263 The above results are sensitive to assumptions about the infectious period and generation time  
264 of SARS-CoV-2. While the qualitative trends and relationships hold regardless, assumptions  
265 of a shorter generation time substantially increase the necessary speed at which activities must  
266 occur to have a meaningful impact (Figures S4 - S8).

## 267 Discussion

268 Test-trace-isolate programs have the potential to play an important role in COVID-19 control,  
269 but the extent of that role depends on each program's ability to limit transmission of the  
270 virus. Here, we have presented a modeling framework with which to evaluate the performance  
271 of test-trace-isolate programs, and shown how four key metrics of performance interact. The  
272 results show that a program's ability to detect cases through community testing is one of the  
273 greatest drivers of program effectiveness, as it is these cases that seed all other activities. Rapid  
274 case isolation, complete contact tracing, and timely quarantine will compound the impact that  
275 identifying a new seed will have on the trajectory of the epidemic. Nevertheless, exceptional  
276 performance may be needed across all of these dimensions if transmission is to be controlled by  
277 test-trace-isolate alone, raising the importance of complementary control activities.

278 Previous work has emphasized the importance of decreasing delays to case isolation and  
279 contact quarantine to reduce disease transmission [20, 21]. However, these models assumed  
280 high testing and isolation coverage ( $\geq 60\%$ ), levels perhaps attainable in the early or late stages  
281 of an outbreak, but far exceeding estimated infection detection rates in many locations with  
282 established epidemics [22–25]. Here, we explore a broader range of case detection and isolation  
283 proportions, including values that may be more feasibly attained in areas with substantial  
284 incidence. In doing so, we show the critical importance of the proportion of cases detected.

285 Once adequate levels of detection are reached, the speed of case isolation and contact quar-  
286 antine will begin to matter more. In practice, these delays are linked, as many of the same  
287 activities must be completed before isolation or quarantine can occur (e.g., sample collection,  
288 laboratory testing, contact of infected or exposed individuals). Hence, practical improvements

289 in important aspects of a test-trace-isolate program, such as speed of laboratory testing, may  
290 have an outsized impact on the performance of the program overall.

291 These results have implications for the design and implementation of test-trace-isolate pro-  
292 grams. The ability to identify and interrupt a high proportion of transmission chains will require  
293 investment in widespread testing. Population screening, in addition to symptom-based or at-will  
294 testing, could meaningfully improve a program's impact on transmission. Inexpensive, easy to  
295 administer, and widely available tests could facilitate expanded detection efforts [26, 27]. Even  
296 if such tests have lower sensitivity, the higher coverage attainable could result in detection of a  
297 higher percentage of infections [28]. Importantly, these improvements to testing capacity and  
298 access must be available to those populations most impacted by COVID-19 and not exacerbate  
299 existing testing disparities. If we increase testing coverage, but fail to reach those who are at  
300 highest risk for infection, there will be little impact on transmission.

301 Any increases in case detection will be ineffective if isolation and quarantine fail to interrupt  
302 transmission. To some extent, this can be counteracted by improvements to other aspects of a  
303 program (e.g., proportion of cases detected), but measures to facilitate effective isolation and  
304 quarantine may be needed to reach transmission control goals. Given the high risk of household  
305 transmission, measures that can intervene in these settings may be highly important. Facilities  
306 for isolation outside of the household were associated with substantial reductions in  $R$  in China  
307 [29]. Use of facial coverings has also been proven effective at reducing household transmission  
308 for SARS-CoV-2 and other respiratory viruses [30–32]. Social and economic support for isola-  
309 tion and quarantine, particularly if outside the home, may be necessary for test-trace-isolate  
310 programs to be effective in many communities [7]. Technology, such as use of mobile phone data  
311 to identify contacts, may improve the speed and completeness of contact tracing, but compli-  
312 ance may be undermined if contact definitions are too broad, and substantial resources would  
313 still be required to initiate and support quarantine of identified contacts [33, 34].

314 The case isolation and contact quarantine completeness metrics used in our model may be  
315 better conceptualized as the *proportion of onward transmission that would have been otherwise*  
316 *caused by those isolated or quarantined*. Thus, programs will see greater reductions in trans-  
317 mission from isolation or quarantine of those who are more likely to transmit. In the expanded  
318 version of our model, we already address differences between symptomatic and asymptomatic  
319 transmission and household versus community contacts. There may be programmatic reasons  
320 to specifically target other groups, and our basic framework could be extended to accommodate  
321 such strategies.

322 Our framework is not without limitations. This model describes a general strategy of tracing  
323 and quarantining the immediate contacts of identified cases in a community. It may not be  
324 easily extensible to settings such as schools or workplaces. Alternative strategies also exist,  
325 including tracing of contacts-of-contacts [35], and so-called backwards tracing [36]. The latter  
326 approach is part of a fundamentally different way of using contact tracing in disease control  
327 that has been used in COVID-19 response in some countries (e.g., Japan [37]), which focuses  
328 on identifying settings that have the potential to facilitate super-spreading events or otherwise  
329 amplify transmission. Our estimates of program effectiveness are sensitive to assumptions of  
330 disease natural history, though we have explored the impact of some of these assumptions

331 (Figures S4 - S8), and further exploration are possible. The model relies on a simplified version  
332 of transmission that does not account for many risk factors for SARS-CoV-2 infection or the  
333 contact structure in the population [35, 38], which could lead to persistent transmission even  
334 when the population reproductive number is low. While the reproductive number is a useful  
335 representation of transmission control at the population level, it does not capture differential  
336 health burden of infections, and a program could have a higher  $R$  but better limit mortality if  
337 it effectively protects at-risk populations.

338 Test-trace-isolate programs should not alone be used to control COVID-19. It is exceedingly  
339 difficult to achieve a reproductive number less than one without additional reductions in trans-  
340 mission from other interventions, which may include masking or broad scale social distancing.  
341 Likewise, our model is based on proportions, but resource needs are determined by the absolute  
342 number of identified cases and traced contacts. When incidence is high, resources needed to  
343 test and trace the desired proportion of infections may be excessive, but if incidence is brought  
344 down through other control measures, the same targets may be logistically feasible. Still, test-  
345 trace-isolate programs need not themselves bring  $R$  below one to be valuable, and incremental  
346 reductions in transmission can alleviate the need for the most severe social distancing measures.

347 Hence, test-trace-isolate programs have a valuable role to play in the COVID-19 re-  
348 sponse, even if such programs themselves are not the whole solution. Understanding the impact  
349 that a program is having, or that would result from investing in better program performance, is  
350 critical to the effective use of these programs within a broader control strategy. We hope that  
351 the model presented here, which is implemented in publicly available tools, will help facilitate  
352 the effective use of these programs in the COVID-19 response.

## 353 Acknowledgments

354 We would like to thank the numerous public health workers and agencies that gave comments  
355 and guidance on the development of our model and the ConTESSA app, including Josh Sharf-  
356 stein and Melissa Marx. We would also like to thank Isabel Rodríguez-Barraquer for her valu-  
357 able comments on this manuscript. Finally, we recognize the valuable support from the Johns  
358 Hopkins Bloomberg School of Public Health Center for Teaching and Learning.

## 359 Funding Statement

360 This work was supported by funding from State of California Institute of Technology (19-13081),  
361 Johns Hopkins Hospital, and Bloomberg Philanthropies.

## 362 References

- 363 1. Zheng, Q. *et al.* HIT-COVID, a global database tracking public health interventions to  
364 COVID-19. *Scientific Data* **7**, 286. <https://doi.org/10.1038/s41597-020-00610-2>  
365 (Dec. 2020).

- 366 2. Desvars-Larrive, A. *et al.* A structured open dataset of government interventions in re-  
367 sponse to COVID-19. *Scientific Data* **7**, 285. [https://doi.org/10.1038/s41597-020-](https://doi.org/10.1038/s41597-020-00609-9)  
368 [00609-9](https://doi.org/10.1038/s41597-020-00609-9) (Dec. 2020).
- 369 3. Nicola, M. *et al.* The socio-economic implications of the coronavirus pandemic (COVID-  
370 19): A review. *International Journal of Surgery* **78**, 185–193. [https://doi.org/10.1016/](https://doi.org/10.1016/j.ijvsu.2020.04.018)  
371 [j.ijvsu.2020.04.018](https://doi.org/10.1016/j.ijvsu.2020.04.018) (June 2020).
- 372 4. United Nations. *Policy Brief: The Impact of COVID-19 on children* (Apr. 2020), 1–17. [https:](https://unsdg.un.org/resources/policy-brief-impact-covid-19-children)  
373 [//unsdg.un.org/resources/policy-brief-impact-covid-19-children](https://unsdg.un.org/resources/policy-brief-impact-covid-19-children).
- 374 5. Wenham, C., Smith, J. & Morgan, R. COVID-19: the gendered impacts of the outbreak.  
375 *The Lancet* **395**, 846–848. <https://doi.org/10.1016/S0140-6736> (Mar. 2020).
- 376 6. Hogan, A. B. *et al.* Potential impact of the COVID-19 pandemic on HIV, tuberculosis, and  
377 malaria in low-income and middle-income countries: a modelling study. *The Lancet Global Health*  
378 **8**, e1132–e1141. [https://doi.org/10.1016/s2214-109x\(20\)30288-6](https://doi.org/10.1016/s2214-109x(20)30288-6) (July 2020).
- 379 7. Burka, D., Steele, L. & Siegler, A. *Covid-19 Contact Tracing Playbook* 2020. [https://](https://contacttracingplaybook.resolvetosavelives.org/)  
380 [contacttracingplaybook.resolvetosavelives.org/](https://contacttracingplaybook.resolvetosavelives.org/).
- 381 8. Abbott, S. *et al.* Estimating the time-varying reproduction number of SARS-CoV-2 using  
382 national and subnational case counts. *Wellcome Open Research* **5**, 112. [https://doi.](https://doi.org/10.12688/wellcomeopenres.16006.1)  
383 [org/10.12688/wellcomeopenres.16006.1](https://doi.org/10.12688/wellcomeopenres.16006.1) (June 2020).
- 384 9. Abbott, S. *et al.* *Covid-19: National and Subnational estimates for the United States of America*  
385 2020. <https://epiforecasts.io/covid/posts/national/united-states/> (2020).
- 386 10. Abbott, S. *et al.* *Covid-19: Estimates for South Korea* 2020. [https://epiforecasts.io/](https://epiforecasts.io/covid/posts/national/south-korea/)  
387 [covid/posts/national/south-korea/](https://epiforecasts.io/covid/posts/national/south-korea/) (2020).
- 388 11. Park, Y. J. *et al.* Contact Tracing during Coronavirus Disease Outbreak, South Korea,  
389 2020. *Emerging infectious diseases* **26**. <https://doi.org/10.3201/eid2610.201315>  
390 (July 2020).
- 391 12. Fraser, C., Riley, S., Anderson, R. M. & Ferguson, N. M. Factors that make an infectious  
392 disease outbreak controllable. *Proc Natl Acad Sci* **101**, 6146–6151. [https://doi.org/](https://doi.org/10.1073/pnas.0307506101)  
393 [10.1073/pnas.0307506101](https://doi.org/10.1073/pnas.0307506101) (Apr. 2004).
- 394 13. *TTI* <https://doi.org/10.5281/ZENODO.4012424>.
- 395 14. *ConTESSA: Contact Tracing Evaluation and Strategic Support Application* [https://iddynamicsjhu.](https://iddynamicsjhu.shinyapps.io/contessa/)  
396 [shinyapps.io/contessa/](https://iddynamicsjhu.shinyapps.io/contessa/).
- 397 15. *Measuring and Maximizing Impact of COVID-19 Contact Tracing — Coursera* [https://](https://www.coursera.org/learn/measuring-and-maximizing-impact-of-covid-19-contact-tracing/)  
398 [www.coursera.org/learn/measuring-and-maximizing-impact-of-covid-19-](https://www.coursera.org/learn/measuring-and-maximizing-impact-of-covid-19-contact-tracing/)  
399 [contact-tracing/](https://www.coursera.org/learn/measuring-and-maximizing-impact-of-covid-19-contact-tracing/).
- 400 16. Madewell, Z. J., Yang, Y., Longini, I. M., Halloran, M. E. & Dean, N. E. Household  
401 transmission of SARS-CoV-2: a systematic review and meta-analysis of secondary attack  
402 rate. *medRxiv*. <https://doi.org/10.1101/2020.07.29.20164590> (July 2020).

- 403 17. Buitrago-Garcia, D. C. *et al.* The role of asymptomatic SARS-CoV-2 infections: rapid  
404 living systematic review and meta-analysis. *medRxiv*. [http://doi.org/10.1101/2020.](http://doi.org/10.1101/2020.04.25.20079103)  
405 [04.25.20079103](http://doi.org/10.1101/2020.04.25.20079103) (July 2020).
- 406 18. Endo, A. *et al.* Estimating the overdispersion in COVID-19 transmission using outbreak  
407 sizes outside China. *Wellcome Open Research* **5**, 67. [https://doi.org/10.12688/](https://doi.org/10.12688/wellcomeopenres.15842.2)  
408 [wellcomeopenres.15842.2](https://doi.org/10.12688/wellcomeopenres.15842.2) (July 2020).
- 409 19. Lloyd-Smith, J. O., Schreiber, S. J., Kopp, P. E. & Getz, W. M. Superspreading and  
410 the effect of individual variation on disease emergence. *Nature* **438**, 355–359. <https://doi.org/10.1038/nature04153> (Nov. 2005).  
411
- 412 20. Hellewell, J. *et al.* Feasibility of controlling COVID-19 outbreaks by isolation of cases and  
413 contacts. *The Lancet Global Health* **8**, e488–e496. [https://doi.org/10.1016/S2214-](https://doi.org/10.1016/S2214-109X(20)30074-7)  
414 [109X\(20\)30074-7](https://doi.org/10.1016/S2214-109X(20)30074-7) (Apr. 2020).
- 415 21. Kretzschmar, M. E. *et al.* Impact of delays on effectiveness of contact tracing strategies  
416 for COVID-19: a modelling study. *The Lancet Public Health* **5**, e452–e459. [https://doi.](https://doi.org/10.1016/S2468-2667(20)30157-2)  
417 [org/10.1016/S2468-2667\(20\)30157-2](https://doi.org/10.1016/S2468-2667(20)30157-2) (Aug. 2020).
- 418 22. Pollán, M. *et al.* Prevalence of SARS-CoV-2 in Spain (ENE-COVID): a nationwide, population-  
419 based seroepidemiological study. *The Lancet* **396**, 535–544. [https://doi.org/10.1016/](https://doi.org/10.1016/S0140-6736(20)31483-5)  
420 [S0140-6736\(20\)31483-5](https://doi.org/10.1016/S0140-6736(20)31483-5) (Aug. 2020).
- 421 23. Xu, X. *et al.* Seroprevalence of immunoglobulin M and G antibodies against SARS-CoV-2  
422 in China. *Nature Medicine* **26**, 1193–1195. [https://doi.org/10.1038/s41591-020-](https://doi.org/10.1038/s41591-020-0949-6)  
423 [0949-6](https://doi.org/10.1038/s41591-020-0949-6) (Aug. 2020).
- 424 24. Stringhini, S. *et al.* Seroprevalence of anti-SARS-CoV-2 IgG antibodies in Geneva, Switzer-  
425 land (SEROCoV-POP): a population-based study. *The Lancet* **396**, 313–319. [https://](https://doi.org/10.1016/S0140-6736(20)31304-0)  
426 [doi.org/10.1016/S0140-6736\(20\)31304-0](https://doi.org/10.1016/S0140-6736(20)31304-0) (Aug. 2020).
- 427 25. Sood, N. *et al.* Seroprevalence of SARS-CoV-2–Specific Antibodies Among Adults in Los  
428 Angeles County, California, on April 10–11, 2020. *JAMA* **323**, 2425. [https://doi.org/](https://doi.org/10.1001/jama.2020.8279)  
429 [10.1001/jama.2020.8279](https://doi.org/10.1001/jama.2020.8279) (June 2020).
- 430 26. Kaplan, E. H. & Forman, H. P. Logistics of Aggressive Community Screening for Coron-  
431 avirus 2019. *JAMA Health Forum* **1**, e200565. [https://doi.org/10.1001/jamahealthforum.](https://doi.org/10.1001/jamahealthforum.2020.0565)  
432 [2020.0565](https://doi.org/10.1001/jamahealthforum.2020.0565) (May 2020).
- 433 27. Shaw, J. New Test Paradigm Needed for SARS-CoV-2. *Harvard Magazine*. [https://](https://harvardmagazine.com/2020/08/covid-19-test-for-public-health)  
434 [harvardmagazine.com/2020/08/covid-19-test-for-public-health](https://harvardmagazine.com/2020/08/covid-19-test-for-public-health) (2020).
- 435 28. Larremore, D. B. *et al.* Test sensitivity is secondary to frequency and turnaround time for  
436 COVID-19 surveillance. *medRxiv*. <https://doi.org/10.1101/2020.06.22.20136309>  
437 (June 2020).
- 438 29. Hao, X. *et al.* Reconstruction of the full transmission dynamics of COVID-19 in Wuhan.  
439 *Nature* **584**, 420–424. <https://doi.org/10.1038/s41586-020-2554-8> (Aug. 2020).
- 440 30. Cowling, B. J. *et al.* Facemasks and hand hygiene to prevent influenza transmission in  
441 households: A cluster randomized trial. *Annals of Internal Medicine* **151**, 437–446. <https://doi.org/10.7326/0003-4819-151-7-200910060-00142>  
442 (Oct. 2009).



- 443 31. Leung, N. H. *et al.* Respiratory virus shedding in exhaled breath and efficacy of face masks.  
444 Nature Medicine **26**, 676–680. <https://doi.org/10.1038/s41591-020-0843-2> (May  
445 2020).
- 446 32. Wang, Y. *et al.* Reduction of secondary transmission of SARS-CoV-2 in households by face  
447 mask use, disinfection and social distancing: a cohort study in Beijing, China. BMJ Global Health  
448 **5**, 2794. <https://doi.org/10.1136/bmjgh-2020-002794> (May 2020).
- 449 33. European Centre for Disease Prevention and Control (ECDC). Mobile applications in  
450 support of contact tracing for COVID-19 – a guidance for EU/EEA member states, 1–  
451 11. [https://www.ecdc.europa.eu/en/publications-data/covid-19-mobile-](https://www.ecdc.europa.eu/en/publications-data/covid-19-mobile-applications-support-contact-tracing)  
452 [applications-support-contact-tracing](https://www.ecdc.europa.eu/en/publications-data/covid-19-mobile-applications-support-contact-tracing) (June 2020).
- 453 34. Kucharski, A. J. *et al.* Effectiveness of isolation, testing, contact tracing, and physical  
454 distancing on reducing transmission of SARS-CoV-2 in different settings: a mathematical  
455 modelling study. The Lancet Infectious Diseases. [https://doi.org/10.1016/s1473-](https://doi.org/10.1016/s1473-3099(20)30457-6)  
456 [3099\(20\)30457-6](https://doi.org/10.1016/s1473-3099(20)30457-6) (June 2020).
- 457 35. Firth, J. A. *et al.* Using a real-world network to model localized COVID-19 control strate-  
458 gies. Nature Medicine, 1–7. <https://doi.org/10.1038/s41591-020-1036-8> (Aug.  
459 2020).
- 460 36. Endo, A. *et al.* Implication of backward contact tracing in the presence of overdispersed  
461 transmission in COVID-19 outbreak. medRxiv, 2020.08.01.20166595. [https://doi.org/](https://doi.org/10.1101/2020.08.01.20166595)  
462 [10.1101/2020.08.01.20166595](https://doi.org/10.1101/2020.08.01.20166595) (Aug. 2020).
- 463 37. Oshitani, H. Cluster-based approach to Coronavirus Disease 2019 (COVID-19) response  
464 in Japan—February–April 2020. Japanese Journal of Infectious Diseases. [https://doi.](https://doi.org/10.7883/yoken.JJID.2020.363)  
465 [org/10.7883/yoken.JJID.2020.363](https://doi.org/10.7883/yoken.JJID.2020.363) (2020).
- 466 38. Wu, C. *et al.* Risk Factors Associated with Acute Respiratory Distress Syndrome and  
467 Death in Patients with Coronavirus Disease 2019 Pneumonia in Wuhan, China. JAMA Internal Medicine  
468 **180**, 934–943. <https://doi.org/10.1001/jamainternmed.2020.0994> (July 2020).